

Stresslog: A python package for modeling wellbore stability in inclined stress states

Arkadeep Ghosh ¹✉

¹ ROCK LAB PRIVATE LIMITED, India ✉ Corresponding author

DOI: [10.21105/joss.08036](https://doi.org/10.21105/joss.08036)

Software

- [Review](#) 
- [Repository](#) 
- [Archive](#) 

Editor: [William Gearty](#)  

Reviewers:

- [@frank1010111](#)
- [@wkearn](#)

Submitted: 12 February 2025

Published: 19 September 2025

License

Authors of papers retain copyright and release the work under a Creative Commons Attribution 4.0 International License ([CC BY 4.0](#)).

Summary

This package is meant to be used by researchers and practitioners working in the field of geomechanics. It uses a collection of algorithms used to iteratively model the state of stress underground, given a well log. The computations use 6 component stress tensor, as calculated using ([Peška & Zoback, 1995](#)), which allows modeling of inclined wellbores in inclined states of stress.

Statement of need

Many commercial packages exist for calculating geomechanical parameters and pressure prediction. Due to their high cost, their usage is limited in research settings. Many practitioners rely on Microsoft Excel for routine geomechanical calculations, but implementing iterative calculations in Excel is challenging.

The python ecosystem for geology is rapidly growing. Handling of well-log and seismic data is now very mature. Geomechanics focused packages exist, such as PyGeoPressure ([Yu, 2018](#)), but this as well as most commercial software assume a vertical stress state.

Stresslog differs from these by aiming to be comprehensive: allowing modeling of variable Biot's coefficient, thermal stresses and inclined stress states, operating on standard well log formats, and with built-in support for log aliasing.

Stresslog has been designed to help with pre-drill, post-drill and realtime geomechanical calculations. It is aimed at empowering researchers with a 1D mechanical earth modeling tool that is freely available and which researchers can modify to apply their own methods when necessary, while allowing practitioners to use industry-standard algorithms to calculate solutions and export well log data.

Stresslog uses welly ([Welly contributors, 2021](#)) to read las files and handle well data. dlisio is used to parse dlis ([Equinor ASA & dlisio contributors, 2025](#)) files. A modified function from lasio ([Inverarity & Lasio contributors, 2023](#)) is used to write las files. Numpy ([Harris et al., 2020](#)), Pandas ([McKinney, 2010](#); [The pandas development team, 2025](#)) and Scipy ([Virtanen et al., 2020](#)) are used for numerical computations. Matplotlib ([Hunter, 2007](#)) and Plotly ([Kruchten et al., 2024](#)) are used for plotting data. Pint is used for unit conversions.

Methodology

To use Stresslog, at the minimum a well log is required containing at least sonic or resistivity or drilling parameters data. Numerous other types of data can be specified to improve/constrain the estimates. Some of the input data require specific format and units to work correctly. Please refer to the documentation for details.

Overburden gradient ([Traugott, 1997](#)), pore-pressure ([Flemings, 2021](#); [Jincai Zhang, 2013](#)), minimum horizontal stress ([Daines, 1982](#); [Mark D. Zoback & Healy, 1992](#)), rock strength ([Horsrud, 2001](#); [Lal, 1999](#)) and other parameters are calculated considering the given well-logging, deviation, and formation data. The maximum horizontal stress is estimated by applying stress-polygon ([M. D. Zoback et al., 2003](#)) for every depth-sample. Borehole image interpretation is considered in the stress-polygon results if available.

The calculation of tilted stress states using the given methodology requires the Euler angles α , β and γ . We calculate the Euler angles from geological data in terms of tilt of the stress tensor, as follows:

$$\text{Tilt Azimuth} = \tan^{-1} \left(\frac{R_{s3,2}}{R_{s3,1}} \right)$$

$$\text{Tilt Angle} = \cos^{-1}(R_{s3,3})$$

Where R_s is the rotation matrix defined by Euler angles α , β and γ , in the NED reference frame.

Considering the azimuth of maximum principal stress as α , the above relations are used to optimize for the angles β and γ . The technique proposed by ([Peška & Zoback, 1995](#)) starts with good estimates of the far field principal stresses, σ_1 , σ_2 and σ_3 , already rotated by the Euler Angles α , β and γ . Usually, however, what is available is an estimate of minimum horizontal stress, an estimate of the vertical stress, and an estimate of maximum horizontal stress. It is insufficient to simply rotate the tensor, as the rotated tensor will not have the correct vertical component. We optimize the principal stresses (σ_1 , σ_2 and σ_3) such that the vertical and horizontal components of the tensor match the specified vertical and horizontal stresses.

For every depth-sample, the stresses resolved on the wellbore wall are calculated along the circumference. The lower critical mudweight is calculated by using the modified Lade formula ([Ewy, 1999](#)) for critical mudweight during this process. A closed-form solution has been derived by setting $\sigma_{\theta_{\min}}$ equal to tensile stress and solving this for the upper critical mud pressure, as follows:

FracturePressure_{non-penetrating} =

$$\left(\begin{aligned} &+ 2 \sigma_{B_{1,1}}'^2 \nu \cos(2\theta_{min}) - 4 \sigma_{B_{1,1}}'^2 \nu \cos(2\theta_{min})^2 + 4 \sigma_{B_{1,1}}' \sigma_{B_{1,2}}' \nu \sin(2\theta_{min}) \\ &- 8 \sigma_{B_{1,1}}' \sigma_{B_{1,2}}' \nu \sin(4\theta_{min}) + 8 \sigma_{B_{1,1}}' \sigma_{B_{2,2}}' \nu \cos(2\theta_{min})^2 + 2 \sigma_{B_{1,1}}' \sigma_{B_{3,3}}' \cos(2\theta_{min}) \\ &- \sigma_{B_{1,1}}' \sigma_{B_{3,3}}' + 2 \sigma_{B_{1,1}}' \nu PP \cos(2\theta_{min}) - 2 \sigma_{B_{1,1}}' \nu \sigma_T \cos(2\theta_{min}) \\ &- 2 \sigma_{B_{1,1}}' \nu TS \cos(2\theta_{min}) - 2 \sigma_{B_{1,1}}' TS \cos(2\theta_{min}) + \sigma_{B_{1,1}}' TS \\ &- 16 \sigma_{B_{1,2}}'^2 \nu \sin(2\theta_{min})^2 + 4 \sigma_{B_{1,2}}' \sigma_{B_{2,2}}' \nu \sin(2\theta_{min}) + 8 \sigma_{B_{1,2}}' \sigma_{B_{2,2}}' \nu \sin(4\theta_{min}) \\ &+ 4 \sigma_{B_{1,2}}' \sigma_{B_{3,3}}' \sin(2\theta_{min}) + 4 \sigma_{B_{1,2}}' \nu PP \sin(2\theta_{min}) - 4 \sigma_{B_{1,2}}' \nu \sigma_T \sin(2\theta_{min}) \\ &- 4 \sigma_{B_{1,2}}' \nu TS \sin(2\theta_{min}) - 4 \sigma_{B_{1,2}}' TS \sin(2\theta_{min}) + 4 \sigma_{B_{1,3}}'^2 \sin(\theta_{min})^2 \\ &- 4 \sigma_{B_{1,3}}' \sigma_{B_{2,3}}' \sin(2\theta_{min}) - 4 \sigma_{B_{2,2}}'^2 \nu \cos(2\theta_{min})^2 - 2 \sigma_{B_{2,2}}'^2 \nu \cos(2\theta_{min}) \\ &- 2 \sigma_{B_{2,2}}' \sigma_{B_{3,3}}' \cos(2\theta_{min}) - \sigma_{B_{2,2}}' \sigma_{B_{3,3}}' - 2 \sigma_{B_{2,2}}' \nu PP \cos(2\theta_{min}) \\ &+ 2 \sigma_{B_{2,2}}' \nu \sigma_T \cos(2\theta_{min}) + 2 \sigma_{B_{2,2}}' \nu TS \cos(2\theta_{min}) + 2 \sigma_{B_{2,2}}' TS \cos(2\theta_{min}) \\ &+ \sigma_{B_{2,2}}' TS + 4 \sigma_{B_{2,3}}'^2 \cos(\theta_{min})^2 - \sigma_{B_{3,3}}' PP \\ &+ \sigma_{B_{3,3}}' \sigma_T + \sigma_{B_{3,3}}' TS + PPTS - \sigma_T TS - TS^2 \end{aligned} \right) \\ \frac{}{2 \sigma_{B_{1,1}}' \nu \cos(2\theta_{min}) + 4 \sigma_{B_{1,2}}' \nu \sin(2\theta_{min}) - 2 \sigma_{B_{2,2}}' \nu \cos(2\theta_{min}) - \sigma_{B_{3,3}}' + TS}$$

where σ'_B is the effective stress tensor in the borehole frame of reference, PP is pore-pressure, TS is tensile strength, ν is Poisson's ratio, σ_T is thermal stress and θ_{min} is the circumferential angle corresponding to minimum hoop stress.

If the user specifies an analysis depth, an orientation-stability plot is calculated at that depth. Synthetic image of the wellbore wall is prepared for 5 metres around the analysis depth. Other plots are also calculated at the analysis depth, including sanding prediction (Willson et al., 2002; J. Zhang et al., 2007).

From observations on multiple wells sampling the same stress field at different wellbore orientations, a better estimate of the stress tensor is possible (Thorsen, 2011).

Case Study

The well data from Equinor Northern Lights dataset (Northern Lights Dataset, 2020) has been used as the example here, to model the stress state occurring in the depth interval of 2600 to 2630m. The resistivity image log shows the occurrence of en-echelon fractures in a vertical wellbore. The model applied here uses parameters similar to (Thompson et al., 2022), with a stress tensor tilt of 2 degrees towards south, and is able to replicate the fracture patterns observed in the actual image log.

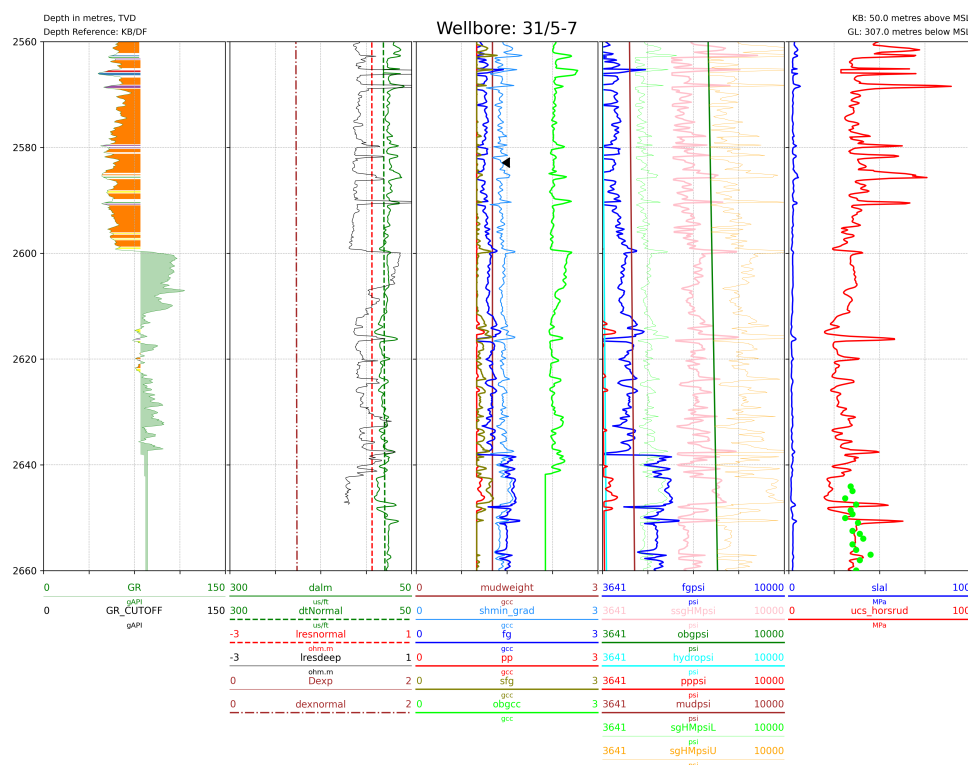


Figure 1: Model of Northern Lights Eos Well showing the Drake I, II and IntraMarine formations.

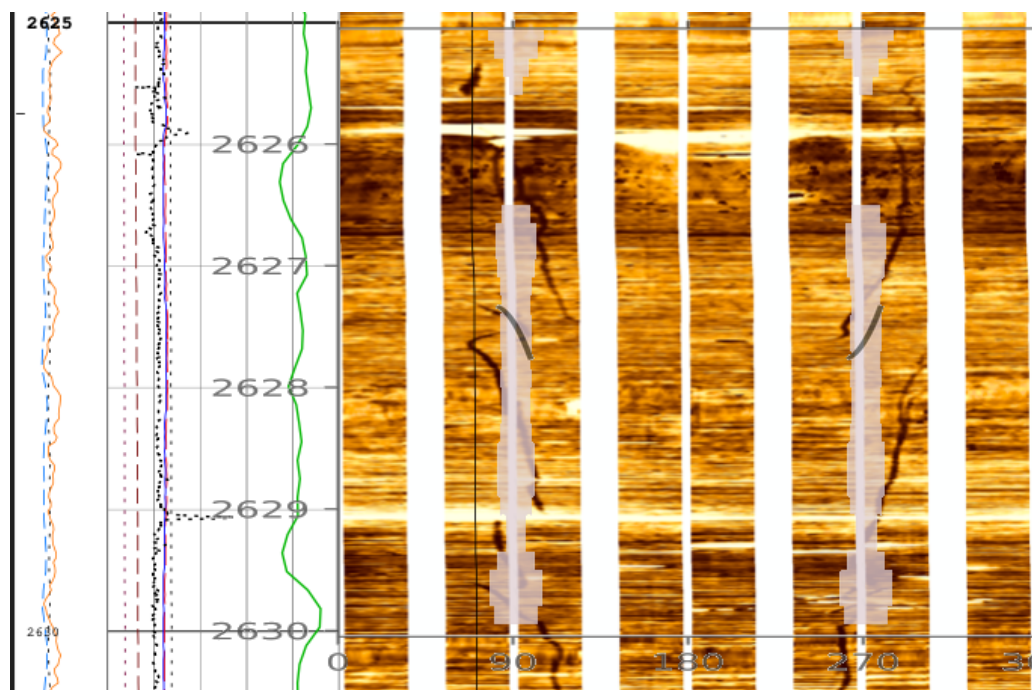


Figure 2: Fracture motifs calculated at 2627.5m and superimposed onto the image log.

It is not being suggested that this interpretation of the data is preferred over any other, the analysis by (Thompson et al., 2022) is much more comprehensive.

Disclosure

No funding/financial support of any form was involved in the creation of this work.

References

- Daines, S. R. (1982). Prediction of fracture pressures for wildcat wells. *Journal of Petroleum Technology*, 34(04), 863–872. <https://doi.org/10.2118/9254-PA>
- Equinor ASA & dlisio contributors. (2025). *Dliso: Python library for working with the well log formats digital log interchange standard (DLIS V1) and log information standard (LIS79)*. <https://github.com/equinor/dliso>
- Ewy, R. T. (1999). Wellbore-stability predictions by use of a modified lade criterion. *SPE Drilling & Completion*, 14(02), 85–91. <https://doi.org/10.2118/56862-PA>
- Flemings, P. B. (2021). Flow focusing and centroid prediction. In *A concise guide to geopressure: Origin, prediction, and applications* (pp. 211–232). Cambridge University Press. <https://doi.org/10.1017/9781107326309.010>
- Harris, C. R., Millman, K. J., Walt, S. J. van der, Gommers, R., Virtanen, P., Cournapeau, D., Wieser, E., Taylor, J., Berg, S., Smith, N. J., Kern, R., Picus, M., Hoyer, S., Kerkwijk, M. H. van, Brett, M., Haldane, A., Fernández del Río, J., Wiebe, M., Peterson, P., ... Oliphant, T. E. (2020). Array programming with NumPy. *Nature*, 585, 357–362. <https://doi.org/10.1038/s41586-020-2649-2>
- Horsrud, P. (2001). Estimating mechanical properties of shale from empirical correlations. *SPE Drilling & Completion*, 16(02), 68–73. <https://doi.org/10.2118/56017-PA>
- Hunter, J. D. (2007). Matplotlib: A 2D graphics environment. *Computing in Science & Engineering*, 9(3), 90–95. <https://doi.org/10.1109/MCSE.2007.55>
- Inverarity, K., & Lasio contributors. (2023). *Lasio* (Version 0.31). <https://github.com/kinverarity1/lasio>
- Kruchten, N., Seier, A., & Parmer, C. (2024). *An interactive, open-source, and browser-based graphing library for python* (Version 5.24.1). <https://doi.org/10.5281/zenodo.14503524>
- Lal, M. (1999). Shale stability: Drilling fluid interaction and shale strength. *SPE Asia Pacific Oil and Gas Conference and Exhibition*, SPE–54356. <https://doi.org/10.2118/54356-MS>
- McKinney, W. (2010). Data structures for statistical computing in python. In S. van der Walt & J. Millman (Eds.), *Proceedings of the 9th python in science conference* (pp. 56–61). <https://doi.org/10.25080/Majora-92bf1922-00a>
- Northern lights dataset: Dataset from NO 31/5-7 (eos) well. (2020). <https://data.equinor.com>
- Peška, P., & Zoback, M. D. (1995). Compressive and tensile failure of inclined well bores and determination of in situ stress and rock strength. *Journal of Geophysical Research: Solid Earth*, 100(B7), 12791–12811. <https://doi.org/10.1029/95jb00319>
- The pandas development team. (2025). *Pandas-dev/pandas: pandas* (Version v2.3.2). Zenodo. <https://doi.org/10.5281/zenodo.16918803>
- Thompson, N., Andrews, J. S., Wu, L., & Meneguolo, R. (2022). Characterization of the in-situ stress on the horda platform – a study from the northern lights eos well. *International Journal of Greenhouse Gas Control*, 114, 103580. <https://doi.org/10.1016/j.ijggc.2022.103580>
- Thorsen, K. (2011). In situ stress estimation using borehole failures — even for inclined stress tensor. *Journal of Petroleum Science and Engineering*, 79(3), 86–100. <https://doi.org/10.1016/j.petrol.2011.07.014>
- Traugott, M. (1997). Pore/fracture pressure determinations in deep water. *World Oil*, 218(8), 68–70.
- Virtanen, P., Gommers, R., Oliphant, T. E., Haberland, M., Reddy, T., Cournapeau, D., Burovski, E., Peterson, P., Weckesser, W., Bright, J., van der Walt, S. J., Brett, M., Wilson, J., Millman, K. J., Mayorov, N., Nelson, A. R. J., Jones, E., Kern, R., Larson, E., ... SciPy 1.0 Contributors. (2020). SciPy 1.0: Fundamental Algorithms for Scientific Computing in Python. *Nature Methods*, 17, 261–272. <https://doi.org/10.1038/s41592-019-0686-2>

- Welly contributors. (2021). *Welly, a python package*. <https://github.com/agilescientific/welly>
- Willson, S. M., Moschovidis, Z. A., Cameron, J. R., & Palmer, I. D. (2002). *New model for predicting the rate of sand production: Vols. All Days* (pp. SPE-78168-MS). <https://doi.org/10.2118/78168-MS>
- Yu, H. (2018). PyGeoPressure: Geopressure prediction in python. *Journal of Open Source Software*, 3(30), 992. <https://doi.org/10.21105/joss.00992>
- Zhang, Jincai. (2013). Effective stress, porosity, velocity and abnormal pore pressure prediction accounting for compaction disequilibrium and unloading. *Marine and Petroleum Geology*, 45, 2–11. <https://doi.org/10.1016/j.marpetgeo.2013.04.007>
- Zhang, J., Standifird, W. B., & Shen, X. (2007). *Optimized perforation tunnel geometry, density and orientation to control sand production: Vols. European Formation Damage Conference* (pp. SPE-107785-MS). <https://doi.org/10.2118/107785-MS>
- Zoback, M. D., Barton, C. A., Brudy, M., Castillo, D. A., Finkbeiner, T., Grollmund, B. R., Moos, D. B., Peska, P., Ward, C. D., & Wiprut, D. J. (2003). Determination of stress orientation and magnitude in deep wells. *International Journal of Rock Mechanics and Mining Sciences*, 40(7), 1049–1076. <https://doi.org/10.1016/j.ijrmms.2003.07.001>
- Zoback, Mark D., & Healy, J. H. (1992). In situ stress measurements to 3.5 km depth in the cajon pass scientific research borehole: Implications for the mechanics of crustal faulting. *Journal of Geophysical Research: Solid Earth*, 97(B4), 5039–5057. <https://doi.org/10.1029/91JB02175>